



Corona based node distribution scheme targeting energy balancing in wireless sensor networks for the sensors having limited sensing range

Richa Mishra¹ · Vivekanand Jha² · Rajeev K. Tripathi¹ · Ajay K. Sharma¹

© Springer Science+Business Media, LLC, part of Springer Nature 2018

Abstract

Wireless sensor networks are equipped with sensor nodes having limited battery as energy source. These sensor nodes have to maintain the desirable coverage of the network to ensure the periodical communication of the sensed data to the base station. Therefore, lifetime of sensor nodes and the energy efficient network coverage are the two major issues that needs to be addressed. Effective placement of wireless sensor nodes is of paramount importance as the lifetime of the network depends upon it. In this work, a corona based energy balanced node deployment scheme for sensors with a limited sensing range is proposed in which the nodes are distributed in accordance with a probability density function (PDF). Optimal number of nodes in each corona is determined using the proposed PDF. Performance of the scheme is evaluated in terms of coverage, energy balance and network lifetime through simulation. The intrinsic characteristic of the proposed PDF has been derived. It is noticed that the node distribution through the proposed scheme not only provides better coverage in each layer but also minimizes both the energy-hole and the coverage-hole problems in the deployment field while maintaining longevity of the sensor network.

Keywords Wireless sensor network · Probability density function · Cumulative density function

1 Introduction

Wireless sensor networks (WSNs) are self-organizing, large-scale networks that are a wireless association of large number of tiny sensor nodes (SNs). These SNs have low battery power, limited storage capacity and low processing speed. These WSNs are being applied in numerous applications such as health monitoring [1], surveillance [2],

temperature monitoring [3], forest [4, 5], battlefield [6], earthquake monitoring [7] and many others. In these applications, the SNs are deployed to operate independently in unattended/attended environments. These SNs sense the data from the surrounding areas and communicate the sensed data to the base station (BS) through multi-hop or single-hop transmission. In WSNs, energy conservation of each node is of utmost importance and also a major challenge. Therefore, the battery of these nodes should be used intelligently to prolong the life of the WSN.

The position of SNs have tremendous impact on the performance of the WSNs. The choice of the node deployment scheme depends upon the metrics such as connectivity of the network [8], full area coverage [9] and remains unchanged throughout the lifetime of the network. A significant problem receiving large consideration recently is the coverage along with connectivity problem [8]. This emphasizes on how effectively the wireless sensors monitor the physical surroundings and also communicate the sensed data to the BS. The area covered by a sensor node is known as its sensing area. When two SNs lie

✉ Richa Mishra
richas.phoenix@gmail.com
Vivekanand Jha
vivekanandjha@igdtuw.ac.in
Rajeev K. Tripathi
rajivtripathi@nitdelhi.ac.in
Ajay K. Sharma
sharmaajayk@nitj.ac.in

¹ National Institute of Technology, Delhi, India

² Indira Gandhi Delhi Technical University for Women, Delhi, India

within the transmission range of each other and can communicate, it can be said that the two nodes are connected. The sensing and communication domain of a SNs are closely related [10]. Therefore, these two parameters are essentially considered in the deployment of SNs in the WSN. Each sensor node dissipates energy in sensing and communicating the data to the BS. Therefore, energy is the most important constraint in WSN. Deployment of SNs and location of the BS has a vital role in increasing the life of the WSN [11, 12]. It is well proven in the literature [13] that multi-hop communication is more energy efficient in terms of lifetime [14, 15] of the network as compared to direct communication. In the case of multi-hop communication the energy depletion rate of nodes placed near the BS is higher as compared to the distant nodes. Energy-hole [16] can be created if the nodes near the BS die out early as compared to the distant nodes. Many researches have been carried out in this area and non-uniform node deployment [12, 16, 17] is considered to be the best strategy to eliminate energy-hole issue. In this type of node deployment maximum numbers of nodes are placed towards the BS and decreases as the distance from the BS increases. These deployed nodes can handle the traffic flow and avoid the energy-hole in WSNs.

In this paper, a non-uniform corona based energy balanced node distribution (ND) scheme is proposed that contributes to better coverage and an energy-efficient communication even when SNs are limited in sensing range [3].

The paper is organized as follows: Sect. 2 discusses the existing literature survey regarding various node deployment schemes. The problem is described in Sect. 3. The energy model is discussed in Sect. 4. Section 5 presents the description of the proposed scheme. Section 6 discusses the EEAGTACO [18] protocol. In Sect. 7, the performance of the proposed scheme is evaluated quantitatively and qualitatively. Finally, Sect. 8 concludes the work done in this paper.

2 Related work

Conserving energy has been fundamental issue in WSNs. Many research have been reported in order to avoid energy-hole problem and maximizing the network lifetime in WSNs. Isabel and Falco in their work [14] discuss about the lifetime of WSN in detail. Here, the authors present the lifetime as a measure of the number of alive nodes, coverage, connectivity, both the connectivity and the coverage and many others. Various parameters that affects the lifetime of WSN are also discussed in their work.

Amini et al. [19] propose a DBS protocol that divides the area into equal sized segments. Different clustering

mechanism were applied to each area in order to reduce the energy consumption by SNs, thereby, increasing the lifetime of the network. Yetgin et al. [15] discuss various techniques that maximizes the lifetime of the network. They are namely: optimal node deployment, routing, data co-relation and many others. We propose a corona based node deployment scheme that not only balances the energy across the network but also provides better coverage and connectivity in WSN thereby maximizes the network lifetime. Hence, the literature is surveyed regarding deployment schemes, network connectivity and coverage in WSN. Rahman et al. [20] classify the deployment scheme into two: non-corona and corona based strategies. The non corona based strategies are distinguished into random Gaussian and random uniform. Here, random means the nodes are dropped by helicopter and uniform means that the nodes density is uniform across the network in deployment field. The authors in [21] use random deployment strategy to deploy SNs. Additional SNs were deployed to achieve maximum coverage. The drawback is the decreased lifetime due to unbalanced energy consumption in the network. In [22], the authors present a mathematical calculation based on which the number of nodes in each corona is placed. Hence, the density of the nodes is decided based on the communication range of each sensor. This approach creates an energy-hole problem in the innermost corona. Similarly, in [23, 24] the authors propose the node deployment scheme with the objective to achieve full coverage with minimum number of SNs. In [25], the authors propose a node deployment scheme that uses the minimum number of nodes and provides full coverage of the network field. However, such an approach cannot be realized in some application such as battle field and habitat monitoring. Halder et al. in their work [26] propose a PDF that derives its intrinsic characteristic such as CDF, expectation and covariance. The authors divide the square region into number of concentric circles. SNs are deployed in accordance with the proposed PDF and is randomly distributed within each annuli. Also, in the considered architecture the number of nodes had decreased as the area had increased.

The work PDFND [27] is an extension of [26]. Here, the questions such as how many number of nodes should be deployed per unit area to accomplish balanced energy consumption in WSN to enhance network lifetime has been answered. Performance has been evaluated by qualitative and quantitative techniques. In [28] the authors demonstrated that the node distribution through Gaussian distribution (GD) was not energy balanced. Further, the authors identified standard deviation as most important parameter for energy balancing. Finally, a node deployment strategy is proposed using customized GD scheme. The authors prove that for a given network, balanced energy

consumption across WSN takes place when SNs are distributed through the customized GD. In this architecture the area of each annulus keeps on increasing and the number of nodes keeps decreasing.

Bhardwaj et al. in their work [29], observed that single-hop transmission to BS consumes more energy compared to multi-hop transmission mechanism. Here, the authors have proposed the optimal size of hop and derived an upperbound in lifetime. Similar work was reported in [30], where the authors argued that equal sized multi-hop transmission was more efficient compared to direct transmission. However, the authors did not prove that equal-sized multi-hop was an optimal criteria. In [31], the network architecture consists of concentric disks with the BS situated at the center. Here, the authors propose a hybrid of single and multi-hop transmissions where the ratio of these two is not equal in a disk. Yuan et al. [13] propose a node distribution scheme to avoid energy-hole problem. Here, the SNs were distributed depending upon the distance from the BS. In this scheme, the energy consumption rate is relatively faster leading to shortening of network lifetime. Chatterjee and Das [9] propose a node distribution strategy to avoid energy-hole in WSN. Here, two types of nodes namely; data originator and data router were considered. Data originators collected the data from the environment and router routes the data to the next hop. This led to increase in network lifetime and reduction in network traffic. Liao et al. [32] proposed a sweep based strategy to balance the energy consumed by the SNs. Liu [33] propose a scheme that adjusts the transmission range of SNs based on inter-nodal distance to maximize WSN lifetime. Ramos et al. [34] introduced the guidelines regarding the node distribution scheme. They showed that the proposed method could increase the network lifetime as well as avoid the energy-hole problem. Ferng et al. [35] in their work, considered a special case in which all the coronas were having uniform width except for the outermost corona.

SNs in WSN may fail to provide the sensed data to BS due to the following reasons namely; depletion of the battery power, poor deployment schemes, physical damage. The failure of the SNs can affect the connectivity amongst the SNs and also to the BS. Our paper provides connectivity among the SNs from one corona to the next intermediate corona. Node failure in any corona may lead to partitioned network due to loss in connectivity in a WSN. Several researchers have proposed various solution for the recovery from the partitioned network. Younis et al. [36] classify the connectivity restoration into three types. In first, the disjoint partition is connected by replacing the failed nodes by the existing SNs. In second,

authors introduce the group of relay nodes to establish the connectivity in a WSN. In third, large number of SNs are deployed to establish k -connectivity [37] to tolerate node failures in WSN. However, the authors do not discuss about achieving the coverage in WSN. In [38], the authors propose a recovery process by moving the relay nodes towards the BS. The communication is established only when all the relay nodes come within the range of each other in order to establish connectivity. Here, the minimum number of relay nodes is obtained using Steiner tree for the disjoint partitioned network. Similar work has been proposed [8]. Here, the authors propose a different optimization technique to calculate the number of relay nodes needed for the restoration of the connectivity in a WSN. Here, the authors do not discuss about the coverage. In [39], the authors propose coverage-aware connectivity method to restore the connectivity along with the coverage of the network. In this method, if a node fails then one of its neighbor is brought to its position to reassure the connectivity and coverage. Wu et al. [40] propose an energy efficient routing scheme called BRIT for sensor nodes distributed in underground tunnel and compare the performance with AODV using various parameters. In [41], the authors analyze the energy consumption and data relay models for their considered architecture. Using the analysis the authors propose ENS-PD algorithm that uses the optimal energy and also prolongs the life of the network. Jha et al. [42] in their work propose a constant area based network architecture. Here the field was partitioned into a number of coronas with the BS positioned at the center. The number of node distribution was non-uniform i.e., the number of nodes distributed kept decreasing in each corona as one moved away from the center. This node distribution may not provide suitable coverage in limited sensing range nodes.

We aim to extend our work discussed in [18]. In this work an energy efficient protocol based on Game Theoretic approach and Ant Colony Optimization (EEAGTACO) was proposed. Here, coalitions amongst SNs were formed based on the coverage and the degree of co-relation in the sensed data throughout the network. In the afore-said work, only the coalition was optimized while the node distribution scheme was yet to be done. Also it was discussed that the EEAGTACO could be used in real life applications such as monitoring the temperature. In such application, the SNs have limited sensing capabilities. In view of this, we propose a corona based node distribution scheme that balances the uniform energy consumption across the network, provides better coverage and connectivity as well as elongates the lifetime of the network even when the SNs have limited sensing capabilities. The main contributions

of this paper are: (1) The PDF is proposed and designed on the basis of node density that controls network lifetime. (2) The energy balanced node deployment algorithm is developed based on the PDF and (3) The performance of the proposed scheme is analysed qualitatively and quantitatively. In qualitative analysis, the intrinsic parameters of the proposed PDF such as CDF and expectations has been derived. Theoretical analysis of energy balancing in WSN is also presented in this section. In quantitative analysis, we compare the proposed ND strategy with other strategies through simulation to substantiate the performance of the algorithm.

3 Problem description

In the literature review section discussed above, the researchers have considered the corona based network architecture wherein the width of each corona is kept uniform. In this architecture, the deployment area is divided into a number of concentric coronas with the BS situated at the center. The width of each corona is kept constant and it is equal to the radius (R) of the innermost corona. Hence, the area of each corona starting from the BS increases in arithmetic progression with the common difference of $2\pi R^2$. In the past various researchers have focused on the approach to avoid the occurrence of energy-hole and coverage-hole in uniform width corona based network architecture. In order to achieve energy efficient WSN, the nodes are distributed in such a way that the node density is inversely proportional to the area of each corona. To avoid the occurrence of energy-holes in the network a non-uniform node distribution is most commonly applied such that the maximum numbers of SNs are deployed in the innermost corona near the BS and thereafter it decreases towards the outer coronas. This type of ND proves to be useful in avoiding the energy-hole problem in WSN. However, for a particular sensing range the number of SNs required to cover the successive coronas should increase from inner corona to outer corona to avoid occurrence of coverage holes. This is because the area of each corona increases in the uniform width corona based network architecture. Hence for avoiding energy-hole, the node density should decrease from inner to outer coronas whereas for avoiding coverage-holes the node density should increase from inner to outer coronas. One important observation is that, these constraints share an inverse relationship with each other with respect to node density. In all these existing approaches it is common that on one hand node density decreases while on other hand the area of each corona increases. Hence, the amalgamation of both the non-uniform ND and the coronas having uniform width

may not provide a suitable choice to avoid both the energy and the coverage hole across the network. Therefore, in this paper we have proposed a ND scheme that considers decreasing width corona based network architecture. In this, when SNs are non-uniformly deployed in decreasing width corona based network architecture, the sensing coverage of the deployed sensor nodes overlap more towards outer coronas as shown in Fig. 1. This brings down the requirements of SNs to be deployed in the outer corona and it also offers better coverage.

The objective of this paper is to propose a non-uniform ND for decreasing width corona based architecture with a constraint of SNs having limited sensing capabilities. An example of SNs having limited sensing capability is well explained in literature [3]. In the proposed varying width corona based network architecture, the deployment area is divided in such a way that the area of each corona decreases as one moves towards the boundary. This type of network architecture for ND can provide better coverage, avoid the occurrence of energy-hole and also balance the energy consumption across the network. Limited sensing range is shown in Fig. 2. Here, R_s and R_c are the sensing and communication range of a SN respectively and S_1 and S_2 are two SNs overlapping an area P_0 . Sensing range is the area sensed by a SN and communication range is the transmission range of a SN.

4 Energy model

The first order radio model similar to [43] has been used in this work. The first energy model consists of a transmitter and a receiver. Here, two kinds of signal loss are used namely; multipath and free space signal loss. When the distance d between the transmitter and the receiver is greater than the threshold d_0 , multipath (mp) signal loss is used while if the distance d between the transmitter and the receptor is less than the threshold d_0 free space (fs) signal loss is used. The threshold d_0 is given by

$$d_0 = \sqrt{\frac{E_{fs}}{E_{mp}}} \quad (1)$$

The multipath and free space signal loss is given by

$$E_{amp} = \begin{cases} E_{fs} \cdot d^2, & \text{if } d < d_0 \\ E_{mp} \cdot d^4, & \text{if } d \geq d_0 \end{cases} \quad (2)$$

Here, E_{amp} , E_{fs} and E_{mp} are the energy used in transmission of fs or mp signal loss, energy consumed in fs signal loss and energy consumed in mp loss respectively. The energy used in transmitting k -bit of data at a distance d is given by

Fig. 1 Sensing overlap in decreasing width network architecture

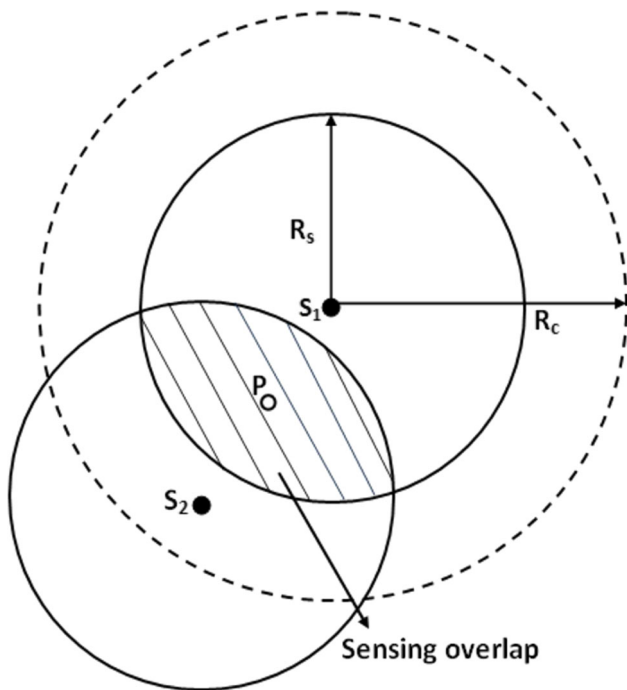
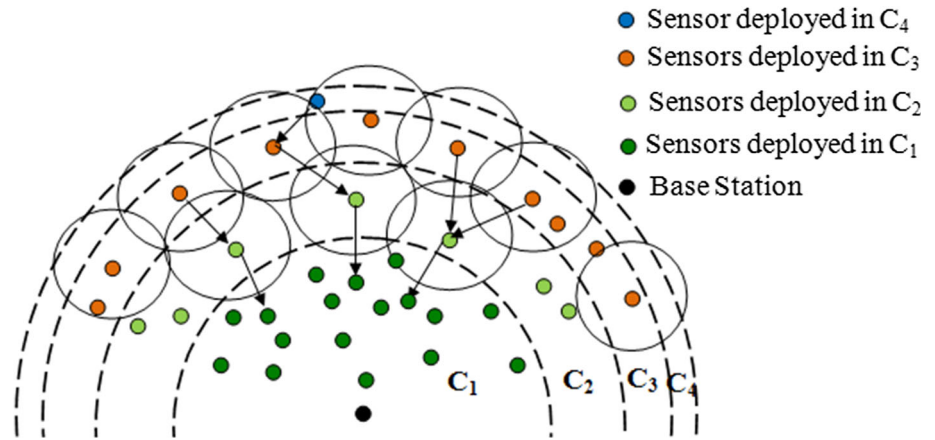


Fig. 2 Communication range greater then sensing range

$$E_{tx}(k, d) = E_{txelec}(k) + E_{txamp}(k, d) \tag{3}$$

Here, E_{tx} , E_{txelec} and E_{txamp} are the energy consumed during transmission of k bits at a distance d , energy consumed by circuitry and the energy consumed in amplification of k -bit data at a distance d . Using Eqs. (2) and (3), the overall energy used up in transmission is given as

$$E_{tx}(k, d) = \begin{cases} kE_{txelec} + kE_{fs}d^2, & \text{if } d < d_0 \\ kE_{txelec} + kE_{mp}d^4, & \text{if } d \geq d_0 \end{cases} \tag{4}$$

Energy consumed in receiving k -bit data is given by

$$E_{rx}(k) = E_{rxelec}(k) = kE_{elec} \tag{5}$$

Here, E_{elec} is the energy required in receiving one-bit data.

5 Proposed solution

The paper proposes a PDF that disseminates sensors with varying densities in the considered deployment/network field to effectively address the problem described in Sect. 3. The deployment field considered is as shown in Fig. 3(a) with the BS situated at the center. The deployment field is divided into a number of concentric circles (NConC). In this division, the innermost corona has the largest area and it decreases in the successive coronas of the deployment field. This kind of division [44] aims to provide better coverage in the network as the maximum number of SNs are deployed in the largest area. Node distribution scheme is proposed based on the designed PDF. Finally, the SNs are disseminated through the proposed node deployment algorithm that distributes the SNs non-uniformly in each corona with the objective of better coverage and elimination of energy-hole thereby, prolonging the life of the network.

5.1 The network model

Considered deployment field is assumed to be square shaped having an area of $M \times M$ units square with BS positioned towards the center of the field as shown in Fig. 3(a). The network field is divided into for equal sized triangles namely; ΔAOB , ΔAOD , ΔBOC and ΔCOD . Initially, the centroid of any triangle can be used in determining the radius of the first corona (C_1). Next, considering C_1 (the centroid of ΔAOB as the new vertex, new ΔAC_1B is formed whose centroid C_2 determines the radius of the next consecutive circle. Same procedure is repeated and the radius of corresponding circles is determined as $R_1, R_2, R_3, \dots, R_L$ as shown in Fig. 3(a).

The radius of each annulus and the number of layers the network should be divided is discussed in detail in [44] and are given as follows:

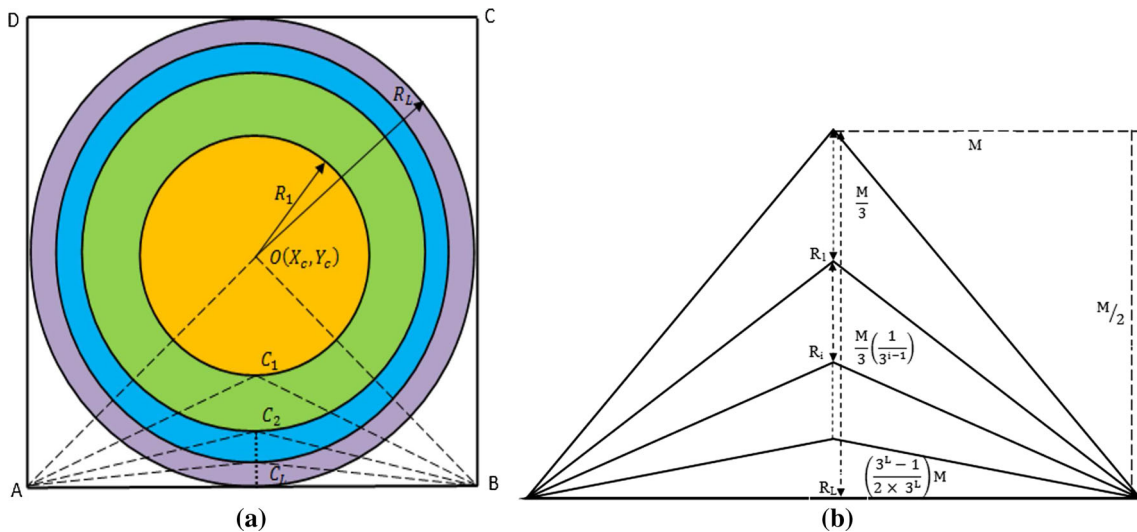


Fig. 3 Network architecture. **a** Proposed network architecture. **b** Successive radii creation

Using the geometrical properties, the distance of i th centroid from the center O is calculated as given by

$$R_i = \frac{(3^i - 1)}{2 \cdot 3^i} M \tag{6}$$

where M and R_i are the length of the side and the radius of the i th concentric circle respectively. Therefore, the total area covered by the i th circle is given as

$$A_i = \pi(R_i^2 - R_{i-1}^2) = \left(\frac{3^i - 2}{3^{2i}}\right) \pi M^2 \tag{7}$$

The detailed description of the division of the deployment field is shown in Fig. 3(b). Here, the number of regions/layers (L) depends on the sensing range (R_s) of a node and the side (M) of the field. Two SNs are known to be redundant [45] if they sense the same area by more than 50% of their total sensing area. Also the two SNs are placed at their optimal positions if their sensing boundaries touch each other. The aforesaid conditions for redundancy (the area covered by two SNs overlap) and optimal placement of SNs are used to find the number of layers in the network. Let the euclidean distance between any two SNs be represented by $|S_1 - S_2|$ then, the situation to bypass the redundancy between these SNs can be expressed by $\frac{R_s}{2} \leq |S_1 - S_2|$. The condition for the optimally placement of SNs can be expressed as $|S_1 - S_2| \leq 2R_s$. Therefore, the placement of the SNs can be expressed by $\frac{R_s}{2} \leq |S_1 - S_2| \leq 2 \times R_s$. Assuming the position of the two SNs are located in adjacent centroid then the above relation can be given as $\frac{R_s}{2} \leq (R_L - R_{L-1}) \leq 2 \times R_s$. Hence according to the principle of optimality the equation can be rewritten and is given by,

$$\frac{3^L}{2} \leq \frac{M}{R_s} < 2 \times 3^L \tag{8}$$

The sensing range of a node is used only to restrict any further divisions of the network.

5.2 Analysis of network lifetime

In EEAGTACO [18] protocol as discussed in Sect. 6, all the nodes form singleton coalition, given the quality service specification (QSS) parameter as $q = 1$. Here singleton coalition refers to coalition having single SN. Therefore in worst case the number of the representative SNs is the same as the total number of SNs distributed in the network. Hence, the analysis has been done on the total number of SNs which is the same as the number of representative SNs in the network and is as discussed below:

Mathematically the lifetime [14, 15] of the i th node can be defined as the ratio of the initial energy of the i th node to its energy consumption rate and is given by

$$LT_i = \frac{E_o}{ECR_i} \tag{9}$$

Here, E_o and ECR_i are the initial energy and energy consumption rate of i th node in the network respectively. Similarly lifetime of j th layer can be obtained by

$$LT_j = \frac{E_o \times T_j}{ECR_j \times T_j} \tag{10}$$

Here, T_j is total number of SNs in j th layer. Therefore, from Eq. (10), it can be said that the lifetime of one layer is same as the lifetime of one node.

Definition 1 Network lifetime is defined as the duration from the beginning of the network till all the SNs in any

corona die out such that an energy-hole is created in the network.

Definition 2 Node density [46] is defined as the ratio of the number of SNs distributed in a corona and the area of that corona.

Data transmission rate (*DTR*) of the *i*th node in the *j*th layer can be defined as the ratio of the data generated in the *i*th layer to the node density in that layer and is mathematically given by

$$DTR_j = \frac{\alpha \times A_j}{\gamma_j \times A_j} = \frac{\alpha}{\gamma_j} \tag{11}$$

Here, α , A_j and γ_j are the data generation rate of a node, area and node density of the *j*th layer respectively. Since the SNs in the *j*th layer transmit their own data along with the data received from (*j* + 1)th layer to the BS or to the next consecutive layer towards the BS, the average DTR of (*j* + 1)th layer towards a node in the *j*th layer is given by

$$DTR_{avg} = \frac{\alpha \gamma_{j+1} A_{j+1}}{\gamma_j A_j} \tag{12}$$

Here, DTR_{avg} , γ_{j+1} and A_{j+1} are the average DTR, the node density and the area of (*j* + 1)th layer respectively.

The node from a layer forward data to the next consecutive layer nearing sink using greedy routing policy [47]. We assume Q-switch [16] routing to forward the data from the outer layer to its inner consecutive layer.

The average data transmission rate of (*j* + 1)th layer is similar to as given in Eq. (12) and is given as $DTR_{j+1} = \frac{\alpha \gamma_{j+1} A_{j+1}}{\gamma_j A_j}$. Therefore, the total data forwarded by a node in the *j*th layer is the sum of the average data transmitted by all the consecutive layers farther away and can be written as

$$DTR_{Total} = \frac{\alpha \sum_{h=j+1}^L \gamma_h A_h}{\gamma_j A_j} \tag{13}$$

Here, L , DTR_{Total} are overall number of layers (NoL), the total data relayed by the outer consecutive layers to its inner successive layer respectively. Using Eqs. (11) and (13), the DTR of each node in the *j*th layer can be obtained by,

$$DTR_j = \begin{cases} \frac{\alpha}{\gamma_j} + \frac{\alpha \sum_{h=j+1}^L \gamma_h A_h}{\gamma_j A_j}, & \text{for } j = 1, 2, \dots, (L - 1) \\ \frac{\alpha}{\gamma_L}, & \text{for } j = L \end{cases} \tag{14}$$

The first component $\frac{\alpha}{\gamma_j}$ is the SNs' own data to be transmitted and the second component $\frac{\alpha \sum_{h=j+1}^L \gamma_h A_h}{\gamma_j A_j}$ is the sum of

all the data of the farther consecutive layers to be transmitted to the innermost layer.

The energy required to transmit SNs' own data is given by

$$E_i = \frac{\alpha}{\gamma_j} \times E_{tx} \tag{15}$$

Here, E_i and E_{tx} is the total energy consumed by the *i*th node and the energy needed to transmit one-bit data respectively. Similarly, the energy needed to transmit the total relayed data from the farther consecutive layers is given by

$$E_{relayeddata} = \left[\frac{\alpha \sum_{h=j+1}^L \gamma_h A_h}{\gamma_j A_j} \right] \times E_{tx} \tag{16}$$

Here, $E_{relayeddata}$ is the total energy consumed to forward all the data from the outer consecutive layers. The energy consumed by each node in *j*th layer is computed using the Eqs. (15) and (16) and is given by

$$ECR_j^{tx} = \begin{cases} \left[\frac{\alpha}{\gamma_j} + \frac{\alpha \sum_{h=j+1}^L \gamma_h A_h}{\gamma_j A_j} \right] \times E_{tx}, & \text{for } j = 1, 2, \dots, (L - 1) \\ \frac{\alpha}{\gamma_L} \times E_{tx}, & \text{for } j = L \end{cases} \tag{17}$$

where ECR_j^{tx} is the energy consumed in transmission by the layer *j*. Similarly, energy consumed in receiving the data from farther consecutive layers is given by

$$ECR_j^{rx} = \left[\frac{\alpha \sum_{h=j+1}^L \gamma_h A_h}{\gamma_j A_j} \right] \times E_{rx} \tag{18}$$

Here, E_{rx} is energy used in receiving data per bit. ECR_j^{rx} is the energy consumed in reception of data by the *j*th layer. Total energy consumed by the *i*th node is given by

$$ECR_i = ECR_i^{tx} + ECR_i^{rx} \tag{19}$$

Here, ECR_i^{tx} , ECR_i^{rx} and ECR_i are the energy consumed in transmission, the energy consumed in reception and the total energy consumed by a node *i* in the layer *j* respectively. Therefore, the total energy consumed by the SNs in *j*th layer is given by

$$ECR_j = \begin{cases} ECR_j^{tx} + ECR_j^{rx}, & \text{for } j = 1, 2, \dots, (L - 1) \\ ECR_L^{tx}, & \text{for } j = L \end{cases} \tag{20}$$

Energy balancing is a situation in which all the SNs in the network use up their energy around like time. Therefore, in order to obtain an energy balanced network the following condition has to be satisfied.

$$ECR_j = ECR_{j+1} = ECR_{j+2} = \dots = ECR_{j+L} \tag{21}$$

Substituting Eqs. (17) and (18) for the layer j and $j + 1$ in the above equation we get

$$\begin{aligned} \frac{\alpha}{\gamma_j} E_{tx} + \left[\frac{\alpha \sum_{h=j+1}^L \gamma_h A_h}{\gamma_j A_j} \right] E_{tx} + E_{rx} \\ = \frac{\alpha}{\gamma_{j+1}} E_{tx} + \left[\frac{\alpha \sum_{h=j+2}^L \gamma_h A_h}{\gamma_{j+1} A_{j+1}} \right] E_{tx} + E_{rx} \end{aligned} \tag{22}$$

On simplifying Eq. (22) we get Eq. (23) and is given by

$$\gamma_j = \gamma_{j+1} \frac{\left[\alpha E_{tx} + (E_{tx} + E_{rx}) \left(\frac{\alpha \sum_{h=j+1}^L \gamma_h A_h}{A_j} \right) \right]}{\left[\alpha E_{tx} + (E_{tx} + E_{rx}) \left(\frac{\alpha \sum_{h=j+2}^L \gamma_h A_h}{A_{j+1}} \right) \right]} \tag{23}$$

The above equation implies that the ratio of node density depends upon two successive layers and the total number of layers. Node density is more towards the BS and decreases in layers further away from BS i.e., $\gamma_j > \gamma_{j+1} > \gamma_{j+2} > \dots > \gamma_N$. When the SNs are distributed according to the said equation, it can be assumed that the SNs in the network deplete their energy at the same time. Now, as the lifetime of a node is defined as $\frac{E_o}{ECR_i}$ where E_o is the initial energy of i th node and ECR_i is the energy dissipation rate of the i th node in the network, replacing ECR_i in denominator in Eq. (9), we get

$$LT_j = \frac{E_o}{ECR_j^{tx} + ECR_j^{rx}} \tag{24}$$

Here, LT_j is the network lifetime of j th layer. Using Eqs. (17), (18), (20) and also substituting the value of A_i in the above equation, the lifetime of the network can be calculated as given by Eq. (25).

$$LT_j = \begin{cases} \frac{E_o \gamma_j \left(\frac{3^j - 2}{3^{2j}} \right)}{\alpha E_{tx} \left(\frac{3^j - 2}{3^{2j}} \right) + \psi \sum_{h=j+1}^L \alpha \gamma_h \left(\frac{3^h - 2}{3^{2h}} \right)}, & \text{for } j = 1, 2, \dots, (L - 1) \\ \frac{E_o \gamma_L}{E_{tx} \alpha}, & \text{for } j = L \end{cases} \tag{25}$$

5.3 Proposed probability density function

The probability density function of a point $P(x, y)$ lying between the annulus $(i - 1)$ and i is given by

$$f(x, y; M, R, i) = \frac{\beta \times (3^i - 2)}{3^{2i-2} \times i} \forall R_{i-1}^2 < x^2 + y^2 \leq R_i^2 \tag{26}$$

The mathematical domain considered in this paper is similar to [44], is divided into L concentric circles centred at $(0, 0)$, each having radius $R_i = \left(\frac{3^i - 1}{2 \times 3^i} \right) \times M$ where M and i are the side of the square field, i is the radius of the i th circle and β is a constant which is given by

$$\beta = \frac{1}{i \times \pi \left(\frac{M}{3} \right)^2 \sum_{i=1}^L \left(\frac{3^i - 2}{3^{2i-2}} \right)^2}$$

Theorem 1 The value of the constant is given by β

$$\beta = \frac{1}{\pi \times \left(\frac{M}{3} \right)^2 \times \left\{ 1 + \frac{1}{2} \left(\frac{7}{9} \right)^2 + \dots + \frac{1}{L^2} \left(\frac{3^L - 2}{3^{2L-2}} \right)^2 \right\}} \tag{27}$$

Theorem 2 If two random discrete variables V and U follow a proposed PDF with parameters i and L , then the CDF of V and U is given as

$$\begin{aligned} F[V \leq x, U \leq y] = \pi \beta \left(\frac{M}{3} \right)^2 \left[\sum_{j=1}^i \left[\frac{1}{j} \left(\frac{3^j - 2}{3^{2j-2}} \right)^2 \right] \right. \\ \left. + \left[\frac{1}{i} \left(\frac{3^i - 2}{3^{2i-2}} \right)^2 - \frac{1}{i} \left(\frac{3^i - 2}{3^{2i-2}} \right)^2 \right] \right] \end{aligned}$$

where (x, y) such that $0 \leq x^2 + y^2 \leq R_\eta^2$, where $i \leq \eta \leq i + 1$.

Theorem 3 If two discrete random variables V and U follow the proposed PDF with parameters l and i then the expectation of V and U is given as

$$E[XY] = \beta 4 \left(\frac{M}{3} \right)^2 \sum_{i=1}^L \left[\frac{81}{4i3^i} + \frac{5103}{2i3^{3i}} - \frac{91}{3^{2i}} \right]$$

The proof of Theorems 1, 2, 3 and also the summary of notations used in this paper is presented in the ‘‘Appendix’’ of the paper.

5.4 PDF based node distribution scheme (PDFNDS)

The proposed PDF is discrete in nature. The objective here is to map the proposed PDF on the layered network architecture as follows: i represents the layer number in both the proposed PDF and layered network field where $i = 1, 2, \dots, L$. Relationship between the radius of the concentric circle and communication radius is $R_i \leq R_c$. The distribution of the sensor node across the network is non-uniform i.e., the number of SNs distributed are maximum near the BS and keeps decreasing as one moves towards the outer annuli. The SNs can be distributed in any inaccessible geographical area [27] through an unmanned helicopter [48–50] in a controlled manner.

The PDF at any point $P(x, y)$ lying between the annulus $(i - 1)$ and i is given as $\frac{\beta(3^i-2)}{3^{2i-2} \times i}$ where $i = 1, 2, \dots, L$. The probability of the number of SNs deployed within an annulus i is given as $\frac{\beta(3^i-2)}{3^{2i-2} \times i} \times A_i$ where A_i is the area of the i th layer. The area of the i th layer is given as $\pi \left(\frac{M}{3}\right)^2 \left(\frac{3^i-2}{3^{2i-2}}\right)$. The value of constant β is given as

$$\beta = \left[\pi \times \left(\frac{M}{3}\right)^2 \times \left\{ \sum_{i=1}^L \frac{1}{i} \left(\frac{3^i-2}{3^{2i-2}}\right)^2 \right\} \right]^{-1}$$

[as given in Eq. (27)]

By replacing A_i , the probability (p_i) of deploying SNs at layer i is given as

$$p_i = \frac{\beta\pi}{i} \left(\frac{3^i-2}{3^{2i-2}}\right)^2 \left(\frac{M}{3}\right)^2 \quad [\text{as given in Equation (47)}]$$

The total number of SNs T_i deployed in the i th layer is given by

$$T_i = p_i \times N_{Total} \tag{28}$$

Here, N_{Total} are the total number of SNs in the deployment field. The node deployment algorithm is given in Algorithm 1.

Algorithm 1 Node Deployment

Input : Area $M \times M$, Center (X_c, Y_c) , Sensing Radius (R_s) , Total number of SNs (N_{Total}) , Sensing radius R_s
Output : Nodes to be disseminated in each corona
 Calculate L from the Equation (8);
for $i = 1$ to L **do**
 Calculate β using Equation (27);
 Calculate p_i from the Equation (49);
 Calculate T_i using Equation (28);
end for

Example Consider a network dimension/area as 100×100 units with $N_{Total} = 250$ and the sensing radius as $R_s = 5$ units is deployed using the proposed node density function based node deployment scheme. The maximum number of layers ' L ' as obtained using Eq. (8) and ' β ' is obtained using Eq. (27) are 4 and 0.00021435 respectively. The probability of the number of SNs deployed in first layer is obtained by replacing i, β, M by 1, 0.00021435 and 250 respectively in Eq. (28). Similarly the probability of the number of SNs to be distributed in the other layers is calculated. The probability of the total number of SNs distributed in the 4-layered network is presented in Table 1. It is observed that the node is distributed according to the designed PDF. As per the design of the PDF, more number of SNs are distributed towards the BS and it decreases in

Table 1 Nodes dissemination

Layers (L_i)	L_1	L_2	L_3	L_4
Probability (p_i)	0.74	0.226	0.023	0.0023
Node distribution (T_i)	224	68	7	1

the layers away from the BS. This kind of deployment is expected to achieve balanced energy consumption, better degree of coverage with each node having limited sensing range thereby, eliminating coverage hole along with the energy efficient node deployment scheme.

6 Node distribution through PDFNDS in EEAGTACO protocol

Implementation of energy efficient approach using game theory and ant colony optimization (EEAGTACO) consists of following phases:

6.1 Node deployment phase

In this phase, the area of the deployment field is divided into coronas as discussed in Sect. 5. The SNs are then

distributed in each corona through PDFNDS scheme as discussed in Algorithm 1.

6.2 Initialization phase

In this phase, the parameters of the SNs such as communication range (R_c), initial energy (E_0), pheromone evaporation rate (ρ), pheromone density of the SNs, negotiation constant (λ), Quality of Service Specification (QSS) (q) and total number of SNs (N_{Total}) are initialized.

6.3 Coalition formation phase

In this phase, coalitions are formed within each corona. All the SNs participate in the formation of coalition. The

coalition initially starts with the formation of singleton coalition. Every node is singleton coalition and declare its partial solution. Singleton coalition is denoted as $s(b, rep)$. Here b is coalition having w SNs in it and rep is the representative node of the coalition. Representative node is the node that communicates with the representative of its successive corona on the behalf of its coalition. All the neighbours of the partial coalitions are discovered and stored for further computation. The size of coalition is extended using ant colony optimization (ACO) [51, 52] technique. All the edges in $s \in \{S\}$, where S is the set of coalitions are identified i.e., $e \in \{E\}$ where E is set all the edge. Now, each edge is chosen probabilistically using the equation given by

$$P(e) = \frac{\tau(e) \cdot \eta}{\sum_{Available\ Edges} \tau(e) \cdot \eta} \quad (29)$$

Here, η is inversely dependent on the distance between the two SNs and τ is evaporation rate of the pheromone. Ant packet is now sent to every $e \in \{E\}$ to discover its next hop neighbour. A negotiation operation is performed between a single node belonging to a coalition $S(b, rep_j)$ and its next hop neighbour ($S(k, rep_j)$). Negotiation operation is performed using utility function computed by

$$U(e_k, b_i) = (|\bar{\sigma} - \sigma|) - \bar{\sigma} \cdot f(d(b_i, e_k), q) \quad (30)$$

Here, σ , $\bar{\sigma}$ and $\bar{\sigma}$ is the standard deviation of the energies of the coalition, the standard deviation calculated after the neighbour node b is added to the coalition and the offset respectively. The $\bar{\sigma}$ is directly proportional to the average residual energy and is calculated by

$$\bar{\sigma} = \lambda * average(E_{Res}) \quad (31)$$

Here, λ is a negotiation constant. The utility function manages two factors; the first component $(|\bar{\sigma} - \sigma|) - \bar{\sigma}$ adds SNs with diverse level of residual energies and the second component $f(d(b_i, e_k), q)$ governs the size of coalition. Here, q is QSS and is defined by the user such as $q = 0.7$ (70% data accuracy). In case of 100 % accurate data i.e., when $q = 1$, all the SNs are singleton coalition. Let X_i and X_c be the data reported by two SNs say, b_i and b_j , then the dissimilarity metric [53] $d(b_i, e_k)$ is given by

$$d(b_i, e_k) = \left| \frac{X_i - X_c}{X_c} \right| \quad (32)$$

Here, $d(b_i, e_k)$ reports the data measured between node b_i and the node which initially started the formation of coalition, let it be denoted by b_c . Accuracy function q is defined by QSS. The data sensed by the SNs using the dissimilarity function should satisfy the Eq. (32). The accuracy function is also called q rule [53] and is given by

$$f(d(b_i, e_k), q) = \begin{cases} 1 - d(b_i, e_k), & d(b_i, e_k) \leq 1 - q \\ -1, & d(b_i, e_k) > 1 - q \end{cases} \quad (33)$$

The value $U(e_k, b_i)$ should be greater than zero i.e., $U(e_k, b_i) > 0$ for the negotiation to be successful. If the negotiation is successful than the ants mark it with pheromone. The pheromone density is computed by

$$\tau_\phi(b_i, e_k) = 1 - \frac{\rho}{e^t} * \tau_\phi \quad (34)$$

Here, $\tau_\phi(b_i, e_k)$, ρ , t and τ_ϕ is the pheromone value associated with the edge joining the edge node e to the neighbour node b , the evaporation rate, the transmission delay of the packet, and the initial pheromone value respectively. Once all the neighbours are discovered, the partial solution is now ready for an optimization phase.

Optimization phase The partial solution and the pheromone deposited (obtained by previous phase) serve as an input to this phase. In this phase, an overall quantity of the pheromone deposited in each coalition is computed. If the pheromone deposited in a coalition is greater than an average value of the pheromone then such a node is selected and added to the optimized coalition. Once a node is part of any optimized coalition it cannot be part of any other optimized coalition.

Association phase In this phase, one node with the highest residual energy from each optimized coalition is elected as a representative node. The representative node from the outer corona sends data to the representative node of its successive inner corona and so on till the message is transmitted to the BS.

7 Results

In this section, the performance analysis of the proposed node deployment scheme is analysed using qualitative and quantitative techniques. Both the qualitative and quantitative analysis is presented here.

7.1 Qualitative analysis

In this sub-section, the theoretic analysis of the balanced energy consumption across the network is evaluated.

7.1.1 Energy balancing

The energy balancing aims to balance the energy consumption of each layer so that the network lifetime of each layer can be maximized. In WSN, the energy balancing is achieved when all the SNs end up their energy at the same time. Similarly, in layered architecture, the energy

balancing is achieved when all SNs in all the layers exhaust their energy at the same time. Nodes deployed in the farthest layer transmit their data to the next consecutive layer towards the BS.

The energy required to transmit the data using Eq. (35) is given as

$$E_{tx}(k, d) = E_{tx_{elec}} k + k E_{tx_{amp}} (R_c^2) \tag{35}$$

The above equation can be rewritten as

$$E_{tx}(k, d) = k E_{Tx} \tag{36}$$

Here, $E_{tx} = E_{tx_{elec}} k + k E_{tx_{amp}} (R_c^2)$. Similarly, energy required to receive k -bit data is given by

$$E_{rx}(k) = k E_{rx_{elec}} = k E_{rx} \tag{37}$$

Here, $E_{rx} = E_{rx_{elec}}$. Energy consumed by the last layer in transmitting its data is given by

$$ECR_L = E_{tx} \times \alpha \times A_L \tag{38}$$

Here, $\alpha \times A_L$ is data to be transmitted by layer L . Rest of the layers transmit their own sensed data and received data from their outer layers. Therefore, energy consumed by layers other than the outer layer is given by

$$ECR_j = E_{tx} \times \alpha \times A_j + \left[(E_{tx} + E_{rx}) \sum_{j=i+1}^L (\alpha \times A_j) \right] \tag{39}$$

To achieve the condition for energy balancing the following condition must be satisfied.

$$\frac{T_1 \times E_o}{ECR_1} = \frac{T_2 \times E_o}{ECR_2} = \dots = \frac{T_i \times E_o}{ECR_i} \tag{40}$$

Here, T_1 and E_o are the number of SNs in the innermost layer and the initial energy of the SNs respectively. From the above Equation, the condition for the balance energy is given as

$$\frac{ECR_i}{T_i} = \frac{ECR_{i+1}}{T_{i+1}} \tag{41}$$

Using Eqs. (39) and (41), we get

$$\frac{T_i}{T_{i+1}} = \frac{E_{tx} \times \alpha \times A_i + \left[(E_{tx} + E_{rx}) \sum_{j=i}^L (\alpha \times A_j) \right]}{E_{tx} \times \alpha \times A_{i+1} + \left[(E_{tx} + E_{rx}) \sum_{j=i+1}^L (\alpha \times A_j) \right]} \tag{42}$$

Substituting A_i by $\left(\frac{3^i - 2}{3^{2i}} \right) \pi M^2$ and by dropping α , we get

$$\frac{T_i}{T_{i+1}} = \frac{E_{tx} \times \alpha \times \left(\frac{3^i - 2}{3^{2i}} \right) \pi M^2 + \left[(E_{tx} + E_{rx}) \sum_{j=i}^L \left(\alpha \times \left(\frac{3^j - 2}{3^{2j}} \right) \pi M^2 \right) \right]}{E_{tx} \times \alpha \times \left(\frac{3^{i+1} - 2}{3^{2i+2}} \right) \pi M^2 + \left[(E_{tx} + E_{rx}) \sum_{j=i+1}^L \left(\alpha \times \left(\frac{3^j - 2}{3^{2j}} \right) \pi M^2 \right) \right]} \tag{43}$$

Simplifying the above equation, we obtain

$$\frac{T_i}{T_{i+1}} = \frac{E_{tx} \times \left(\frac{3^i - 2}{3^{2i}} \right) + \left[(E_{tx} + E_{rx}) \sum_{j=i}^L \left(\frac{3^j - 2}{3^{2j}} \right) \right]}{E_{tx} \times \left(\frac{3^{i+1} - 2}{3^{2i+2}} \right) + \left[(E_{tx} + E_{rx}) \sum_{j=i+1}^L \left(\frac{3^j - 2}{3^{2j}} \right) \right]} \tag{44}$$

By using the proposed PDF discussed in Sect. 5, the LHS of the above expression can be written as

$$\frac{T_i}{T_{i+1}} = \frac{(3^i - 2)^2 3^{4i+2} (i + 1)}{(3^{i+1} - 2)^2 3^{4i-2} i} \tag{45}$$

Equating the above Eqs. (44) and (45), we get

$$\frac{E_{tx} \times \left(\frac{3^i - 2}{3^{2i}} \right) + \left[(E_{tx} + E_{rx}) \sum_{j=i}^L \left(\frac{3^j - 2}{3^{2j}} \right) \right]}{E_{tx} \times \left(\frac{3^{i+1} - 2}{3^{2i+2}} \right) + \left[(E_{tx} + E_{rx}) \sum_{j=i+1}^L \left(\frac{3^j - 2}{3^{2j}} \right) \right]} = \frac{(3^i - 2)^2 3^{4i+2} (i + 1)}{(3^{i+1} - 2)^2 3^{4i-2} i} \tag{46}$$

Assuming E_{tx} and E_{rx} as constant in the above equation, we get $LHS \simeq RHS$. Hence, the objective of energy balancing is fulfilled with the proposed node distribution deployed using the proposed scheme.

7.2 Quantitative analysis

Simulation parameters and its meaning is as given in Table 2. We have used MATLAB for simulations. The SNs are assumed to be static. The performance of the proposed probability density function based node distribution scheme (PDFNDS) is compared to the node distribution as given in PDFND [27] and EEAGTACO protocol [18].

7.2.1 Analysis of PDFNDS

Analysis of the proposed node distribution scheme has been carried out in Fig. 4(a). Here, the number of SNs distributed is plotted against the number of layers. It can be seen that with the total SNs $N_{Total} = 50$, a total of 39 SNs are deployed in *layer-1* and it keeps decreasing in the outer successive layers as one moves towards the boundary in 3 – *layer* network. Similar is the case with $N_{Total} = 100$, $N_{Total} = 150$, $N_{Total} = 200$ and $N_{Total} = 250$. In the

Table 2 Simulation parameter and its meaning

Parameter symbol	Meaning	Value
Area (M)	Deployment area	100–300 square units
Nodes (T_{Total})	Sensor SNs to be deployed	100–300
E_o	Initial energy	0.01 units
R_s	Sensing range	4–8 units

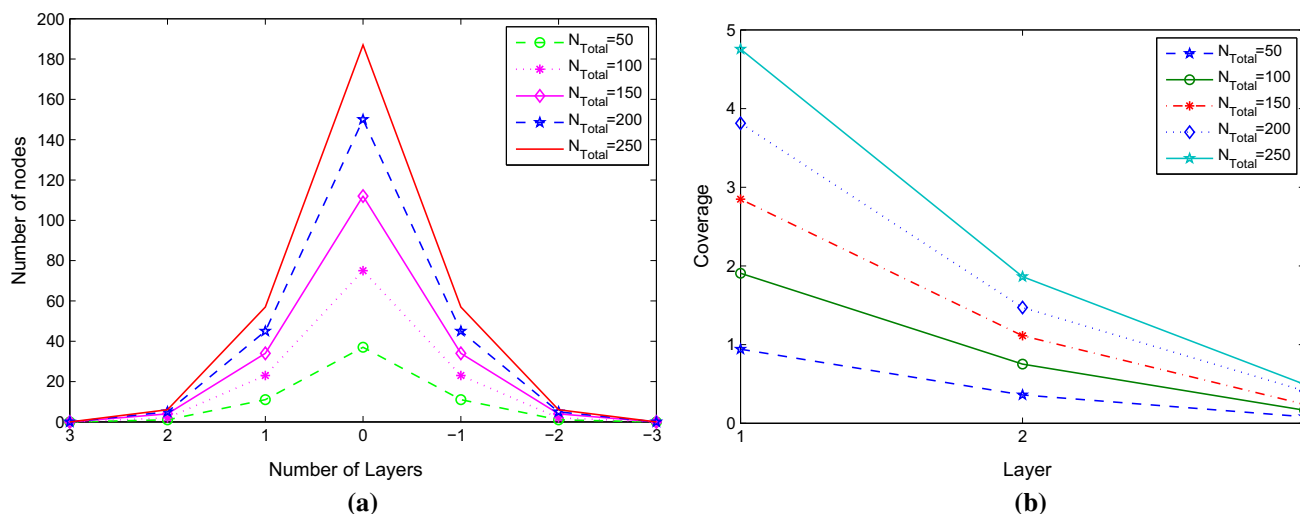


Fig. 4 Analysis of PDFNDS. **a** Node distribution through PDFNDS. **b** Coverage achieves using PDFNDS

proposed scheme, the node distribution is directly proportional to the deployment area.

Coverage analysis of the node distribution through PDFNDS is carried out using the definition given below.

Definition 3 The coverage density of i th layer is defined as the sensing area of the SNs multiplied by the number of SNs deployed per unit area in that layer.

Therefore using the above definition of coverage we get $L^i_{Coverage} = \frac{T_i \times \pi \times R_s^2}{A_i}$. Substituting A_i in the above equation of coverage as given above we get $\frac{T_i \times \pi \times R_s^2}{\frac{3^{2i} \times T_i \times R_s^2}{M^2 \times (3^i - 2)}} = \frac{3^{2i} \times T_i \times R_s^2}{M^2 \times (3^i - 2)}$. Here,

$L^i_{Coverage}$ is the coverage obtained in i th layer. In Fig. 4(b) coverage obtained is plotted against the number of layers. It is observed that when the SNs are distributed through PDFNDS scheme, 1-coverage [54] is achieved with $N_{Total} = 50$ while k -coverage is achieved with $N_{Total} = 100, N_{Total} = 150, N_{Total} = 200$ and $N_{Total} = 250$ in case of layer-1. A gradual decrease in the curve towards layer-3 is noticed in the figure. This is because the distribution of SNs is dependent on the area of each layer. In other words, as the area of each successive annulus decreases as one moves towards the boundary so does the distribution of SNs. Therefore, higher coverage density is achieved in the layer innermost layer and it keeps decreasing as one progresses towards the boundary. Similar

and predictable behaviour is noticed for all the considered cases when $N_{Total} = 50, N_{Total} = 100, N_{Total} = 150, N_{Total} = 200$ and $N_{Total} = 250$.

Coverage obtained in various layers in 4-layered network architecture with varying sensing range (R_s) is shown in Fig. 5. The nodes having different sensing range such as $R_s = 4, R_s = 5, R_s = 6, R_s = 7$ and $R_s = 8$, are distributed using the proposed scheme and their coverage in various layers is examined. It is noticed that when the SNs are equipped with $R_s = 4$ the coverage density obtained in layer-1 is 2.1 and it keeps decreasing in successive outer annuli i.e., layer-2, 3 respectively. Similar is the case with $R_s = 5, 6, 7$ and 8. Therefore, it can be said that higher the sensing range of the node, higher is the coverage density achieved in the network.

7.2.2 Comparison of proposed scheme with the existing scheme

Proposed node distribution scheme is compared with the node distribution scheme discussed in PDFND [27].

Area covered, node density achieved and number of SNs distributed is plotted on y-axis while number of layers is plotted on x-axis is shown in Fig. 6. In the proposed scheme (PDFNDS), the area covered by layer-1 is maximum while it decreases as one approaches towards the

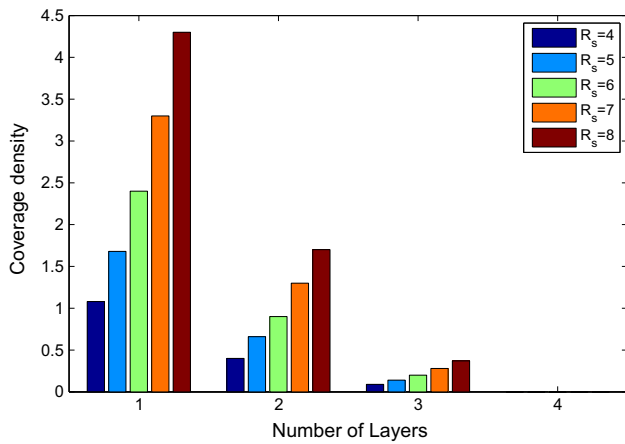


Fig. 5 Coverage obtained with varying sensing range of nodes

boundary of the deployment field. Also, the maximum number of SNs are deployed towards the BS and it decreases as one moves towards the boundary of the deployment field. It can be verified from the figure that the maximum area is covered by *layer-1* and also maximum number of SNs are distributed in this area. Also the coverage density achieved through the PDFNDS is approximately 20 units. Similar is the case with other 2 layers namely; *layer-2* and *layer-3*. Area covered by *layer-3* is smaller as compared to *layer-1* and 2. The number of SN distribution is directly proportional to the deployment area, hence the number of SNs distributed is lesser as compared to other layers. It can be verified from the Fig. 6(a). Node distribution through the PDFND is shown in Fig. 6(b). In this scheme, the area is divided in such a way that the larger area is towards the boundary and it decreases in geometric progression. Also, the number of SNs distributed

is inversely proportional to the deployment area i.e., maximum number of SNs are distributed in *layer-1* when compared to the node distribution in *layer-2* and *layer-3* as observed from the figure. The maximum number of SNs are deployed in *layer-1* therefore, maximum coverage density is obtained in *layer-1* when compared to the other cases. Comparing the two node distribution schemes, it can be said that the proposed scheme offers better coverage density in larger area.

The lifetime of the EEAGTACO protocol is analyzed in the Fig. 7(a). Here, the number of dead SNs for each round is plotted. It is observed from the figure that the node distribution through PDFNDS improves the performance of EEAGTACO protocol. The representative SNs from each coalitions in the outer corona send the data to the representative node to its consecutive inner corona on behalf of its coalition members. This node distribution scheme reduces the number of transmissions thereby increases the lifetime of the network. The figure for the number of representative SNs in each round is shown in Fig. 7(b). The gradual curve is noticed when the SNs are distributed through PDFPDS whereas a steep curve is noticed in case of EEAGTACO protocol. It can be seen from the figure that the performance of EEAGTACO protocol is increased when the SNs are distributed through PDFNDS scheme.

Finally, the lifetime of the network in terms of balanced energy consumption is analyzed in the Fig. 8. Here, the number of dead SNs in plotted against the number of rounds for PDFNDS and PDFND. A steep curve is noticed when the SNs are distributed though PDFND while a gradual curve is obtained when the SNs are distributed through PDFNDS respectively. The SNs deployed through

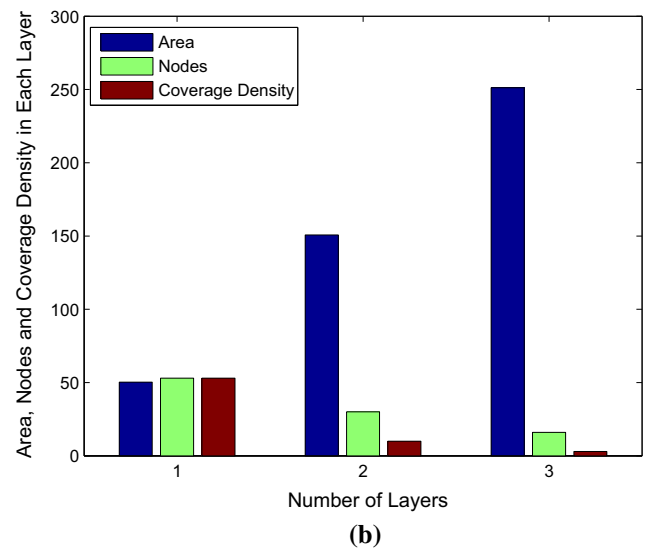
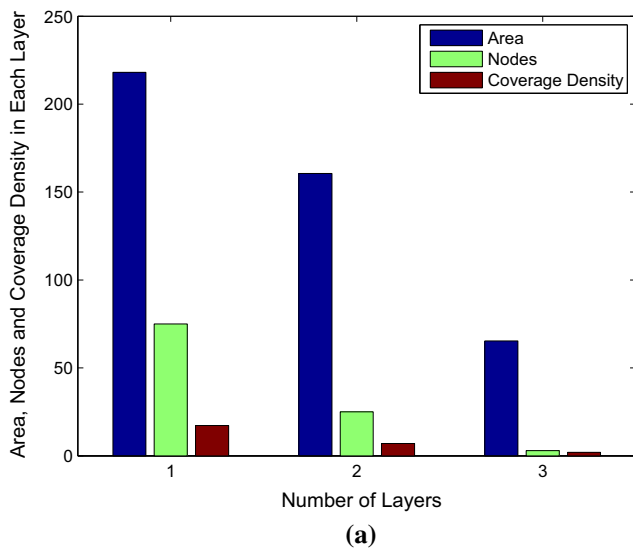


Fig. 6 Comparison of node distribution schemes. a Node distribution through PDFNDS. b Node distribution through PDFND

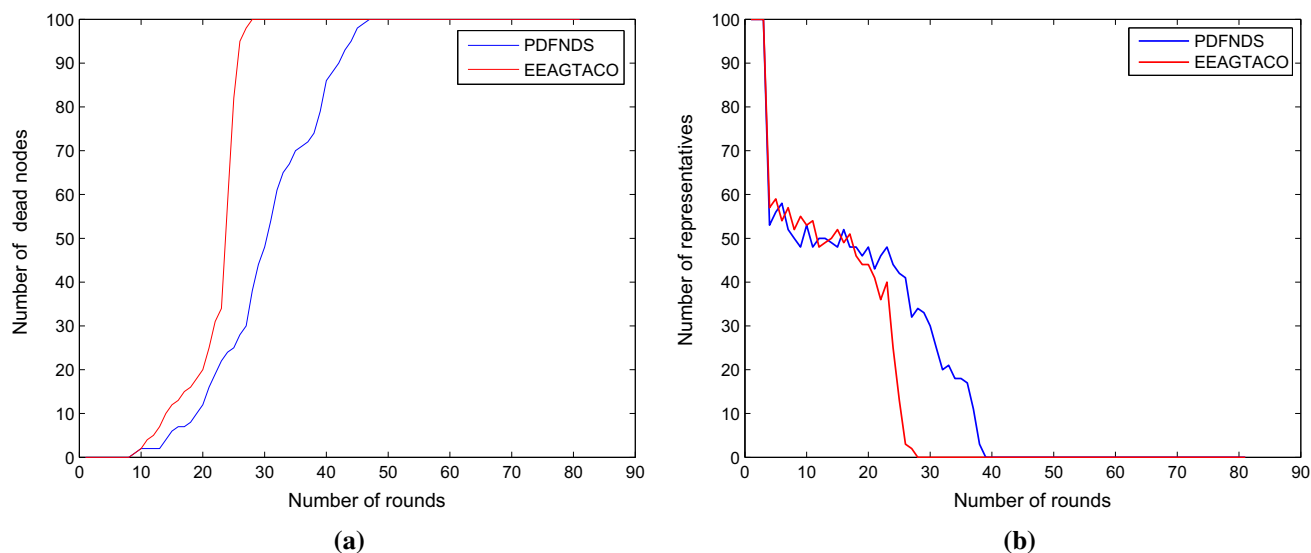


Fig. 7 Comparison of lifetime and number of representatives. **a** Comparison of Lifetime. **b** Number of representatives in each round

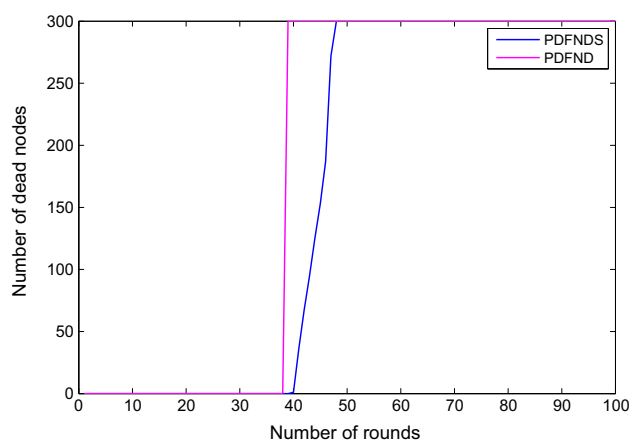


Fig. 8 Comparison of lifetime for balanced energy consumption

the PDFNDS increases the lifetime of the network when compared with the node distribution through PDFND. The gradual decay in number of SNs in case of PDFNDS is due to the proposed mathematical model for the area division and inter-layer communication from the outermost to the innermost layer. With parameter $R_s = 4$, the deployment area is divided into 13 layers. Number of layers is obtained using the relation $\frac{M}{2 \times R_s}$ where M is the side of the deployment field and R_s is the sensing range of the node. The SNs are then distributed using their proposed scheme. With $N_{Total} = 300$, the number of SNs distributed in each layer is 117, 66, 36, 22, 15, 11, 8, 6, 5, 4, 4, 3 and 3. It can be seen that the SNs distributed in last layers is equal. The SNs distributed in the inner layers have to receive the data coming from the outer layer, generate its own data and finally aggregate the total data to forward it to the next consecutive layer. Due to this, more number of SNs should

be distributed in the inner layers. But in case of PDFND, the energy-hole is created in *layer2-1*. Due to this the network is partitioned into two sub-networks. Similar problem occurs in *layer-10*. Therefore, there are three partitions in the network in this case. It can be concluded that when the SNs are distributed using PDFND, the energy-hole is created when the SNs have smaller sensing range. This leads to decrease in the lifetime of the network using our definition of lifetime. In the case of PDFNDS, the SNs are distributed in such a way that energy-hole is eliminated, thereby maintaining the connectivity. This increases the network lifetime as shown in Fig. 8.

8 Conclusion

Corona based energy balanced node distribution scheme employing PDF for WSNs is proposed. The considered WSN field in the proposed work is divided into a number of coronas with BS positioned at the center of the deployment field. The area of each corona keeps decreasing as one move away from the BS towards the boundary of the deployment field. The corona based energy balanced node distribution in accordance with the designed PDF is then proposed. The objective of the proposed scheme is to provide energy balancing in each corona, eliminate energy-hole and minimize coverage-hole problems in the WSN field. The performance of the proposed scheme is compared with the existing techniques and analysed qualitatively. It is observed that the scheme not only balances the energy across the network but also minimized and eliminates coverage and energy-hole problems. The proposed

scheme is especially designed for the applications in which sensors have limited sensing range.

Appendix

Summary of notations used in the paper is given below (Table 3):

The proof of Theorem 1 is as given below:

Let p_i denote the probability of a point (x, y) lying between the annulus i and $(i - 1)$. From the proposed probability density function, the probability p_i is given by

$$p_i = \frac{\beta \times (3^i - 2)}{i \times 3^{2i-2}} \iint f(x, y) dx dy \tag{47}$$

Here, $\iint f(x, y) dx dy$ is the domain area. The considered domain area is circular and is given as

$$\iint f(x, y) dx dy = \pi \times \left(\frac{M}{3}\right)^2 \times \left(\frac{3^i - 2}{3^{2i-2}}\right) \tag{48}$$

By the fundamental law of probability,

$$\sum_{i=1}^L p_i = 1 \text{ or } \frac{\beta \times (3^i - 2)}{i \times 3^{2i-2}} \times \pi \times \left(\frac{M}{3}\right)^2 \times \left(\frac{3^i - 2}{3^{2i-2}}\right) = 1$$

Substituting Eq. (48) in Eq. (47),

Table 3 Table of notations

Notation	Meaning
E_{tx}	Energy consumed during transmission
E_{rx}	Energy consumed in reception
$O(X_c, Y_c)$	Center of the network domain
R_i	Radius of the i th corona
$M \times M$	Area of the network domain in square units
L	Number of layer
C_i	i th corona of the network domain
α	Data generation rate
γ	Node density
ECR	Energy consumption rate
DTR	Data transmission rate
E_o	Initial energy of nodes
T_j	Total nodes in j th layer
A_j	Area of j th layer
β	A constant
p_i	Probability of nodes in i th layer
N_{Total}	Total number of nodes to be deployed
R_c	Communication range of a node
R_s	Sensing range of a node

$$p_i = \frac{\beta \times (3^i - 2)}{i \times 3^{2i-2}} \times \pi \times \left(\frac{M}{3}\right)^2 \times \left(\frac{3^i - 2}{3^{2i-2}}\right) \tag{49}$$

Simplifying the above equation using the fundamental law of probability we get,

$$\beta = \frac{1}{\pi \times \left(\frac{M}{3}\right)^2 \times \left\{1 + \frac{1}{2} \left(\frac{7}{9}\right)^2 + \dots + \frac{1}{L^2} \left(\frac{3^L - 2}{3^{2L-2}}\right)^2\right\}}$$

The proof of Theorem 2 is as given below:

The probability of discrete random variable X and Y for any value within a range i is given as

$$\pi \beta \left(\frac{M}{3}\right)^2 \sum_{j=1}^i \frac{1}{j} \left(\frac{3^j - 2}{3^{2j-2}}\right)^2 \tag{50}$$

The probability of the variable X and Y between domain area A_i and A_η such that $\eta > i$ is given as

$$\frac{\beta}{i} \left[A_\eta - A_i \right] \tag{51}$$

Substituting value of A_i and A_η in the above equation we get

$$\frac{\beta}{i} \left[\pi \left(\frac{M}{3}\right)^2 \left(\frac{3^\eta - 2}{3^{2\eta-2}}\right)^2 - \pi \left(\frac{M}{3}\right)^2 \left(\frac{3^i - 2}{3^{2i-2}}\right)^2 \right] \tag{52}$$

Simplifying the above equation we get

$$\pi \left(\frac{M}{3}\right)^2 \frac{\beta}{i} \left[\left(\frac{3^\eta - 2}{3^{2\eta-2}}\right)^2 - \left(\frac{3^i - 2}{3^{2i-2}}\right)^2 \right] \tag{53}$$

The CDF of X and Y using Eqs. (50) and (53) is obtained as

$$F[X \leq x, Y \leq y] = \pi \beta \left(\frac{M}{3}\right)^2 \left[\sum_{j=1}^i \left[\frac{1}{j} \left(\frac{3^j - 2}{3^{2j-2}}\right)^2 \right] + \left[\frac{1}{i} \left(\frac{3^\eta - 2}{3^{2\eta-2}}\right)^2 - \frac{1}{i} \left(\frac{3^i - 2}{3^{2i-2}}\right)^2 \right] \right]$$

The proof of the Theorem 3 as is given below:

Expectations of two random variables X and Y is given as

$$E[XY] = E_1[XY] + E_1[XY] + \dots + E_L[XY] = \sum_{i=1}^L E_i[XY] \tag{54}$$

Here, $E_i[XY]$ is the expectation of X and Y in domain i . Now,

$$E_i[XY] = \iint f(xy) x y dy dx \tag{55}$$

$$E_i[XY] = \frac{\beta}{i} \iint x y dy dx \tag{56}$$

$$E_i[XY] = \frac{4\beta}{i} \left[\int_{x=0}^{x=R_{i-1}} x \left(\int_{y=\sqrt{R_{i-1}^2-x^2}}^{y=\sqrt{R_1^2-x^2}} y dy \right) dx + \int_{x=R_{i-1}}^{x=R_i} x \left(\int_{y=0}^{y=\sqrt{R_1^2-x^2}} y dy \right) dx \right] \quad (57)$$

Simplifying the above equation we get,

$$E_i[XY] = \beta \left(\frac{M}{3} \right)^4 \left[\frac{81}{4i3^i} + \frac{5103}{2i3^{3i}} - \frac{91}{32i} \right] \quad (58)$$

Substituting the above equation in Eq. (54), we get

$$E[XY] = \beta 4 \left(\frac{M}{3} \right)^2 \sum_{i=1}^L \left[\frac{81}{4i3^i} + \frac{5103}{2i3^{3i}} - \frac{91}{32i} \right]$$

References

- Biagetti, G., Crippa, P., Falaschetti, L., Orcioni, S., & Turchetti, C. (2016). Wireless surface electromyograph and electrocardiograph system on 802.15.4. *IEEE Transactions on Consumer Electronics*, 62(3), 258–266.
- Mishra, R., Kumar, P., Chaudhury, S., & Indu, S. (2013). Monitoring a large surveillance space through distributed facematching. In *2013 fourth national conference on computer vision, pattern recognition, image processing and graphics(NCVPRIPG)* (pp. 1–5). December 2013.
- Mathew, J., Hauser, C., Stoll, P., Kenel, C., Polyzos, D., Havermann, D., et al. (2017). Integrating fiber fabry-perot cavity sensor into 3-d printed metal components for extreme high-temperature monitoring applications. *IEEE Sensors Journal*, 17(13), 4107–4114.
- Tanenbaum, A. S., Gamage, C., & Crispo, B. (2006). Taking sensor networks from the lab to the jungle. *Computer*, 39(8), 98–100.
- Meng, S., Kashyap, S. R., Venkatramani, C., & Liu, L. (2012). Resource-aware application state monitoring. *IEEE Transactions on Parallel and Distributed Systems*, 23(12), 2315–2329.
- Dempsey, T., Sahin, G., Morton, Y. T., & Hopper, C. M. (2009). Intelligent sensing and classification in ad hoc networks: A case study. *IEEE Aerospace and Electronic Systems Magazine*, 24(8), 23–30.
- Lin, S. C., Alshehri, A. A., Wang, P., & Akyildiz, I. F. (2017). Magnetic induction-based localization in randomly deployed wireless underground sensor networks. *IEEE Internet of Things Journal*, 4(5), 1454–1465.
- Joshi, Y. K., & Younis, M. (2016). Restoring connectivity in a resource constrained WSN. *Journal of Network and Computer Applications*, 66, 151–165.
- Chatterjee, P., & Das, N. (2014). Coverage constrained non-uniform node deployment in wireless sensor networks for load balancing. In *2014 applications and innovations in mobile computing (AIMoC)* (pp. 126–132). February 2014.
- Zhu, Chuan, Zheng, Chunlin, Shu, Lei, & Han, Guangjie. (2012). Review: A survey on coverage and connectivity issues in wireless sensor networks. *Journal of Network and Computer Applications*, 35(2), 619–632.
- Anastasi, Giuseppe, Conti, Marco, Di Francesco, Mario, & Passarella, Andrea. (2009). Energy conservation in wireless sensor networks: A survey. *Ad Hoc Networks*, 7(3), 537–568.
- Liu, A., Jin, X., Cui, G., & Chen, Z. (2013). Deployment guidelines for achieving maximum lifetime and avoiding energy holes in sensor network. *Information Sciences*, 230, 197–226. (Mobile and Internet Services in Ubiquitous and Pervasive Computing Environments.).
- Yuan, J., Ling, Q., Yan, J., Zhang, W., & Gu, H. (2011). A novel non-uniform node distribution strategy for wireless sensor networks. In *2011 Chinese control and decision conference (CCDC)* (pp. 3737–3741). May 2011.
- Dietrich, I., & Dressler, F. (2009). On the lifetime of wireless sensor networks. *ACM Transactions on Sensor Networks*, 5(1), 5:1–5:39.
- Yetgin, H., Cheung, K. T. K., El-Hajjar, M., & Hanzo, L. H. (2017). A survey of network lifetime maximization techniques in wireless sensor networks. *IEEE Communications Surveys Tutorials*, 19(2), 828–854. (Secondquarter 2017).
- Wu, X., Chen, G., & Das, S. K. (2008). Avoiding energy holes in wireless sensor networks with nonuniform node distribution. *IEEE Transactions on Parallel and Distributed Systems*, 19(5), 710–720.
- Lian, J., Naik, K., & Agnew, G. B. (2006). Data capacity improvement of wireless sensor networks using non-uniform sensor distribution. *International Journal of Distributed Sensor Networks*, 2(2), 121–145.
- Mishra, R., Jha, V., Tripathi, R. K., & Sharma, A. K. (2017). Energy efficient approach in wireless sensor networks using game theoretic approach and ant colony optimization. *Wireless Personal Communications*, 95(3), 3333–3355.
- Amini, N., Fazeli, M., Miremadi, S. G., & Manzuri, M. T. (2007). Distance-based segmentation: An energy-efficient clustering hierarchy for wireless microsensor networks. In *Fifth annual conference on communication networks and services research (CNSR'07)* (pp. 18–25). May 2007.
- Rahman, A. U., Alharby, A., Hasbullah, H., & Almuzaini, K. (2016). Corona based deployment strategies in wireless sensor network. *Journal of Network and Computer applications*, 64(C), 176–193.
- Ishizuka, M., & Aida, M. (2004). Performance study of node placement in sensor networks. In *24th international conference on distributed computing systems workshops, 2004. Proceedings* (pp. 598–603). March 2004.
- Rahman, I. A. A. U., Al-Shomrani, M. M., & Hasbullah, H. (2015). Two echelon architecture using relay node placement in wireless sensor network. *Journal of Applied Sciences*, 5, 214–222.
- Ammari, H. M., & Das, S. (2010). A study of k-coverage and measures of connectivity in 3D wireless sensor networks. *IEEE Transactions on Computers*, 59(2), 243–257.
- Gupta, H. P., & Rao, S. V. (2016). Demand-based coverage and connectivity-preserving routing in wireless sensor networks. *IEEE Systems Journal*, 10(4), 1380–1389.
- Zaidi, S. A. R., Hafeez, M., Khayam, S. A., Mclernon, D. C., Ghogho, M., & Kim, K. (2009). On minimum cost coverage in wireless sensor networks. In *2009 43rd annual conference on information sciences and systems*, (pp. 213–218). March 2009.
- Halder, S., Ghosal, A., Chaudhuri, A., & DasBit, S. (2011). *A probability density function for energy-balanced lifetime-enhancing node deployment in WSN* (pp. 472–487). Berlin: Springer.
- Halder, S., & DasBit, S. (2014). Design of a probability density function targeting energy-efficient node deployment in wireless

- sensor networks. *IEEE Transactions on Network and Service Management*, 11(2), 204–219.
28. Halder, S., & Ghosal, A. (2014). Is sensor deployment using Gaussian distribution energy balanced? In *2014 IEEE 11th consumer communications and networking conference (CCNC)* (pp. 721–728). January 2014.
 29. Bhardwaj, M., Garnett, T., & Chandrakasan, A. P. (2001). Upper bounds on the lifetime of sensor networks. In *ICC2001. IEEE international conference on communications. Conference record (Cat. No. 01CH37240)* (Vol. 3, pp. 785–790).
 30. Mhatre, V., & Rosenberg, C. (2004). Design guidelines for wireless sensor networks: Communication, clustering and aggregation. *Ad Hoc Networks*, 2(1), 45–63.
 31. Efthymiou, C., Nikolettseas, S., & Rolim, J. (2004). Energy balanced data propagation in wireless sensor networks. In *18th international parallel and distributed processing symposium, 2004. Proceedings.* (p. 225). April 2004.
 32. Liao, Wen-Hwa, Kuai, Ssu-Chi, & Lin, Mon-Shin. (2015). An energy-efficient sensor deployment scheme for wireless sensor networks using ant colony optimization algorithm. *Wireless Personal Communications*, 82(4), 2135–2153.
 33. Liu, X. (2015). An optimal-distance-based transmission strategy for lifetime maximization of wireless sensor networks. *IEEE Sensors Journal*, 15(6), 3484–3491.
 34. Ramos, H. S., Boukerche, A., Oliveira, A. L., Frery, A. C., Oliveira, E. M., & Loureiro, A. A. (2016). On the deployment of large-scale wireless sensor networks considering the energy hole problem. *Computer Networks*, 110, 154–167.
 35. Ferng, H. W., Hadiputro, M., & Kurniawan, A. (2011). Design of novel node distribution strategies in corona-based wireless sensor networks. *IEEE Transactions on Mobile Computing*, 10(9), 1297–1311.
 36. Younis, M., Senturk, I. F., Akkaya, K., Lee, S., & Senel, F. (2014). Topology management techniques for tolerating node failures in wireless sensor networks: A survey. *Computer Networks*, 58, 254–283.
 37. Han, X., Cao, X., Lloyd, E. L., & Shen, C. C. (2010). Fault-tolerant relay node placement in heterogeneous wireless sensor networks. *IEEE Transactions on Mobile Computing*, 9(5), 643–656.
 38. Lee, S., & Younis, M. (2010). Recovery from multiple simultaneous failures in wireless sensor networks using minimum Steiner tree. *Journal of Parallel and Distributed Computing*, 70(5), 525–536.
 39. Tamboli, N., & Younis, M. (2009). Coverage-aware connectivity restoration in mobile sensor networks. In *2009 IEEE international conference on communications* (pp. 1–5). June 2009.
 40. Wu, D., Li, R., & Bao, L. (2008). A holistic routing protocol design in underground wireless sensor networks. In *2008 The 4th international conference on mobile ad-hoc and sensor networks* (pp. 187–194). December 2008.
 41. Luo, J., Di, W., Pan, C., & Zha, J. (2015). Optimal energy strategy for node selection and data relay in WSN-based IoT. *Mobile Networks and Applications*, 20(2), 169–180.
 42. Jha, V., Verma, S., Prakash, N., & Gupta, G. (2018). Corona based optimal node deployment distribution in wireless sensor networks. *Wireless Personal Communications*, 102, 325–354.
 43. Heinzelman, W. R., Chandrakasan, A., & Balakrishnan, H. (2000). Energy-efficient communication protocol for wireless microsensor networks. In *Proceedings of the 33rd annual Hawaii international conference on system sciences* (Vol. 2, pp. 10). January 2000.
 44. Mishra, R., Jha, V., Tripathi, R. K., & Sharma, A. K. (2018). Design of probability density function targeting energy efficient network for coalition based wsns. *Wireless Personal Communications*, 99(2), 651–680.
 45. Bhattacharjee, M., & Gupta, S. (2014). Determining redundant nodes in a location unaware wireless sensor network. In *2014 IEEE international conference on advanced communications, control and computing technologies* (pp. 858–862) May 2014.
 46. Li, J., & Mohapatra, P. (2007). Analytical modeling and mitigation techniques for the energy hole problem in sensor networks. *Pervasive and Mobile Computing*, 3(3), 233–254.
 47. Xian, Q., & Long, Y. (2016). An enhanced greedy perimeter stateless routing algorithm for wireless sensor network. In *2016 IEEE international conference of online analysis and computing science (ICOACS)* (pp. 181–184). May 2016.
 48. Bernard, M., Kondak, K., Maza, I., & Ollero, A. (2011). Autonomous transportation and deployment with aerial robots for search and rescue missions. *Journal of Field Robotics*, 28(6), 914–931.
 49. Song, W. Z., Huang, R., Xu, M., Shirazi, B., & LaHusen, R. (2010). Design and deployment of sensor network for real-time high-fidelity volcano monitoring. *IEEE Transactions on Parallel and Distributed Systems*, 21(11), 1658–1674.
 50. Mathisen, S. H., Grindheim, V., & Johansen, T. A. (2017). Approach methods for autonomous precision aerial drop from a small unmanned aerial vehicle. *IFAC-PapersOnLine*, 50(1), 3566–3573. (20th IFACWorld Congress).
 51. Kyriakopoulos, C. A., Papadimitriou, G. I., Nicopolitidis, P., & Varvarigos, E. (2016). Energy-efficient lightpath establishment in backbone optical networks based on ant colony optimization. *Journal of Lightwave Technology*, 34(23), 5534–5541.
 52. Dorigo, M., & Stützle, T. (2004). *Ant colony optimization*. Scituate: Bradford Company.
 53. Voukaidis, A. C., Anastasopoulos, M. P., & Cottis, P. G. (2013). Energy efficiency in wireless sensor networks: A game-theoretic approach based on coalition formation. *ACM Transactions on Sensor Networks*, 9(4), 43:1–43:27.
 54. Huang, C.-F., & Tseng, Y.-C. (2005). The coverage problem in a wireless sensor network. *Mobile Networks and Applications*, 10(4), 519–528.



Richa Mishra is currently working as an Assistant Professor in the Department of Computer Science and Engineering in National Institute of Technology Delhi, Delhi, India. She has received B.E. degree from Shivaji University Kolhapur, India and M.E. degree from University of Mumbai, India in the year 2008. She has completed her Ph.D. from National Institute of Technology Delhi, Delhi, India in the year 2018. She has served 5 years as

an Assistant Professor in Guru Gobind Singh Indraprastha University (GGSIU) and Delhi Technological University (Formerly known as Delhi College of Engineering), India. Her current area of interest includes designing energy efficient protocols in wireless sensor networks.



Vivekanand Jha received the B.Tech. degree in Computer Science & Information Technology (CSIT) from I.E.T Bareilly, Rohilkhand University, U.P, India, in 2001 and the M.Tech. degree in Information Technology from Indian Institute of Information Technology, Gwalior, India, in 2006. He is working as Assistant Professor in Department of Computer Science & Engineering at Indira Gandhi Delhi Technical University for Women, Delhi,

India from 2007. His research interests include wireless sensor networks, Algorithm Design, and Cloud Computing.



Rajeev K. Tripathi received Ph.D. degree from Indian Institute of Technology, Kanpur, India. He is currently working as an Assistant Professor in Electronics and Communication Engineering at National Institute of Technology, Delhi, India. His current area of interest includes clustering algorithms for Wireless Sensor Networks.



Ajay K. Sharma is working as Director at National Institute of Technology (An Institute of National Importance), Ministry of Human Resource Development, Government of India, New Delhi since October 2013. He received his B.E. in Electronics and Electrical Communication Engineering from Punjab University Chandigarh, India in 1986, M.S. in Electronics and Control from Birla Institute of Technology (BITS), Pilani in the year 1994 and

Ph.D. in Electronics Communication and Computer Engineering in

the year 1999. His Ph.D. thesis was on “Studies on Broadband Optical Communication Systems and Networks”. After serving various organizations from 1986 to 1995, he has joined National Institute of Technology (Erstwhile Regional Engineering College) Jalandhar as Assistant Professor in the Department of Electronics and Communication Engineering in the year 1996. From November 2001, he has worked as Professor in the ECE department and thereafter he has worked as Professor in Computer Science & Engineering from 2007 to 2013 in the same institute. His major areas of interest are broadband optical wireless communication systems and networks, dispersion compensation, fiber nonlinearities, optical soliton transmission, WDM systems and networks, Radio-over-Fiber (RoF) and wireless sensor networks and computer communication. He has published 290 research papers in the International/National Journals/Conferences and 12 books. He has supervised 22 Ph.D. and 52 M.Tech. theses. He has completed two R&D projects funded by Government of India and one project is ongoing. He was associated to implement the World Bank project of 209 Million for TEQIP-I programme of the institute. He has been appointed as member of technical Committee on Telecom under International Association of Science and Technology Development (IASTD) Canada for the term 2004–2007 and he is Life Member of Optical Society of America, USA, (LM ID-361253), Computer Society of India, Mumbai, India, (LM-Associate: 01099298), Advanced Computing & Communications Society, Indian Institute of Science, Bangalore, India, (L284M1100306), SPIE, USA, (ID: 619838), Indian Society for Technical Education (I.S.T.E.), New Delhi, India, (LM-11724), Fellow The Institution of Electronics and Telecommunication Engineers (IETE), (F-224647).